Supporting Information

Yb,Nd,Er-Doped Upconversion Nanoparticles: 980 nm versus 808 nm Excitation

Lisa M. Wiesholler[a†], Florian Frenzel[b,c†], Bettina Grauel[b,c], Christian Würth[b] , Ute Resch-Genger[b] and Thomas Hirsch[a]

[a] University of Regensburg, Institute of Analytical Chemistry, Chemo- and Biosensors, 93040 Regensburg, Germany. E-mail: thomas.hirsch@ur.de

[b] BAM Federal Institute for Materials Research and Testing, Division 1.10 Biophotonics, 12489 Berlin, Germany, E-mail: ute.resch@bam.de

[c] WG Nanooptics, Institute for Physics, Humboldt-University Berlin, Newtonstraße 15, 12489 Berlin, Germany.

† These authors contributed equally.

Table of Contents

1. Synthesis of Upconversion Nanoparticles

Synthesis of hexagonal core particles $NaYF_4$:20%Yb,2%Er

For the synthesis of 1 mmol β-$NaYF_4$:20%Yb,2%Er particles, the lanthanide chlorides were dissolved in methanol (5 mL) in the corresponding molar ratios. Oleic acid (8 mL) and 1-octadecene (15 mL) was added into a 50 mL three necked round bottom flask under nitrogen flow. This solution was heated to 160 °C and vacuum was applied for 30 min unless it appeared clear. This solution was cooled to room temperature and 4.00 mmol NH_4F and 2.5 mmol NaOH in 10 mL methanol were added and then the suspension was kept at 120 °C for 30 min before heating to reflux (ca. 320 °C). The heating-time was controlled by the appearance of upconversion luminescence in the synthesis flask upon continuous excitation with a 980 nm laser module (200 mW, cw). When the upconversion luminescence can be identified by the bare eye, the solution is kept at reflux for additional 8 min. To achieve a complete transformation of the nanocrystals from the α- to the β-from and to receive monodisperse particles, a heating time of 15 min turned out to be best for the 25 nm sized particles. To obtain particles with bigger diameters the heating steps and the reflux time was adapted. The particles were precipitated by the addition of excess of ethanol and collected by centrifugation at 1,000 g for 5 min. The precipitate was washed with chloroform/ethanol (1:10 v/v) two times and five times with cyclohexane/acetone (1:10 v/v) by repeated redispersion-precipitation-centrifugation cycles. In the end, for removing aggregates, the particles were dispersed in 10 mL cyclohexane, centrifuged at 1,000 g for 3 min and the supernatant was collected.

Synthesis of cubic $NaYF_4$:5%Yb,5%Nd; $NaYF_4$:10%Yb,10%Nd; $NaYF_4$:15%Yb,15%Nd; $NaYF_4$:10%Yb and $NaYF_4$

Cubic shell-precursor materials were synthesized via a synthesis protocol almost identical to the synthesis of hexagonal $NaYF_4$:Yb,Er particles, by using the respective molar ratios of the lanthanide chlorides. The suspension was not heating to reflux but kept for 30 min at 240 °C to receive the cubic crystal lattice. Moreover, the purification of the particles was performed as described above.

Synthesis of core-shell $NaYF_4$:20%Yb,2%Er@$NaYF_4$:5-15%Yb,5-15%Nd; $NaYF_4$:20%Yb,2%Er@$NaYF_4$:10%Yb; $(Yb@Yb,Nd)^{is}$; $(Yb@Yb)^{is}$; $(Yb)^{is2}$; $(Yb)^{is5}$

The core particles ($NaYF_4$:20%Yb,2%Er) together with the respective shell precursors ($NaYF_4$:10%Yb,10%Nd, or $NaYF_4$:10%Yb, or $NaYF_4$) were filled in different ratios according to the desired thickness of the shell into 50 mL three necked round bottom flasks and were kept under nitrogen flow. For the 4 nm shell a ratio core to precursor material of 1 to 3, while for the 2 nm shell a ratio of 1 to 1.5 was used. Per 1 mmol total content of core $NaYF_4$-particles, 5 mL oleic acid and 5 mL 1-octadecene were added. After this the β-$NaYF_4$-particles and the precursors were separately heated to 100 °C before vacuum was applied for 1 h unless a clear solution was obtained. After this the β-$NaYF_4$-particles were heated to reflux and the shell precursor was kept under nitrogen flow at 100 °C. Every 10 minutes a small portion (approx. 1 - 3 mL) of the shell precursor was added to the mixture. When the precursor material was consumed, the solution was kept for another 10 min at reflux. The precipitation and

purification of the core-shell nanoparticles was performed according to the protocol described for redispersion-precipitation cycles of $NaYF_4$:20%Yb,2%Er.

2. ICP-Characterization of all Particle Systems

Table S1. ICP-MS-data showing the composition of all particle systems used in this study.

[1]These values are calculated.

particle system		core			active-shell			inert-shell	total[1]			
	acronym	Y^{3+}/%	Yb^{3+}/%	Er^{3+}/%	Y^{3+}/%	Yb^{3+}/%	Nd^{3+}/%	Y^{3+}/%	Y^{3+}/%	Yb^{3+}/%	Nd^{3+}/%	Er^{3+}/%
β-$NaYF_4$:20%Yb,2%Er@ $NaYF_4$:5%Yb,5%Nd@$NaYF_4$	-	77.6 ± 0.17	20.6 ± 0.21	1.8 ± 0.04	89.1 ± 0.17	5.9 ± 0.18	4.9 ± 0.01	-	74.1 ± 0.17	23.2 ± 0.12	2.0 ± 0.11	0.7 ± 0.01
β-$NaYF_4$:20%Yb,2%Er@ $NaYF_4$:10%Yb,10%Nd@$NaYF_4$	$(Yb@Yb,Nd)^{is}$	77.6 ± 0.17	20.6 ± 0.21	1.8 ± 0.04	80.2 ± 0.29	10.0 ± 0.16	9.8 ± 0.09	99.8 ± 0.20	78,5 ± 0.50	14.0 ± 0.14	6.5 ± 0.05	1.0 ± 0.02
β-$NaYF_4$:20%Yb,2%Er@ $NaYF_4$:15%Yb,15%Nd@$NaYF_4$	-	77.6 ± 0.17	20.6 ± 0.21	1.8 ± 0.04	69.3 ± 0.10	15.1 ± 0.13	15.6 ± 0.10	-	68.6 ± 0.15	18.8 ± 0.07	12.0 ± 0.04	0.6 ± 0.02
β-$NaYF_4$:20%Yb,2%Er @$NaYF_4$:10%Yb@$NaYF_4$	$(Yb@Yb)^{is}$	77.6 ± 0.17	20.6 ± 0.21	1.8 ± 0.04	89.1 ± 0.75	10.9 ± 0.11	-	98.7 ± 0.13	84.2 ± 0.51	14.8 ± 0.06	-	1.0 ± 0.00
β-$NaYF_4$20%Yb,2%Er@$NaYF_4$	$(Yb)^{is5}$	77.6 ± 0.17	20.6 ± 0.21	1.8 ± 0.04	-	-	-	99.0 ± 0.10	89.8 ± 0.8	9.2 ± 0.54	-	1.0 ± 0.01
β-$NaYF_4$:20%Yb,2%Er@$NaYF_4$	$(Yb)^{is2}$	77.6 ± 0.17	20.6 ± 0.21	1.8 ± 0.04	78.4 ± 0.57	19.4 ± 0.32	2.2 ± 0.00	100.0 ± 0.00	80.4 ± 0.32	17.5 ± 0.23	-	2.1 ± 0.01
α-$NaYF_4$:5%Yb,5%Nd	-				90.5 ± 0.17	5 ± 0.02	4.5 ± 0.01					
α-$NaYF_4$:10%Yb,10%Nd	-				79.1 ± 0.14	9.9 ± 0.07	10 ± 0.07					
α-$NaYF_4$:15%Yb,15%Nd	-				70 ± 0.10	15 ± 0.13	15 ± 0.10					
α-$NaYF_4$:10%Yb					90.1 ± 0.20	9.9 ± 0.08						
α-$NaYF_4$:20%Yb,2%Er	-	78.1 ± 0.15	19.9 ± 0.10	2.0 ± 0.03	77.6 ± 0.17							
α $NaYF_4$	-							100 ± 0.4				

3. Characterization of Core-Shell $NaYF_4$:Yb,Er@$NaYF_4$:5-15%Yb,5-15%Nd Particles

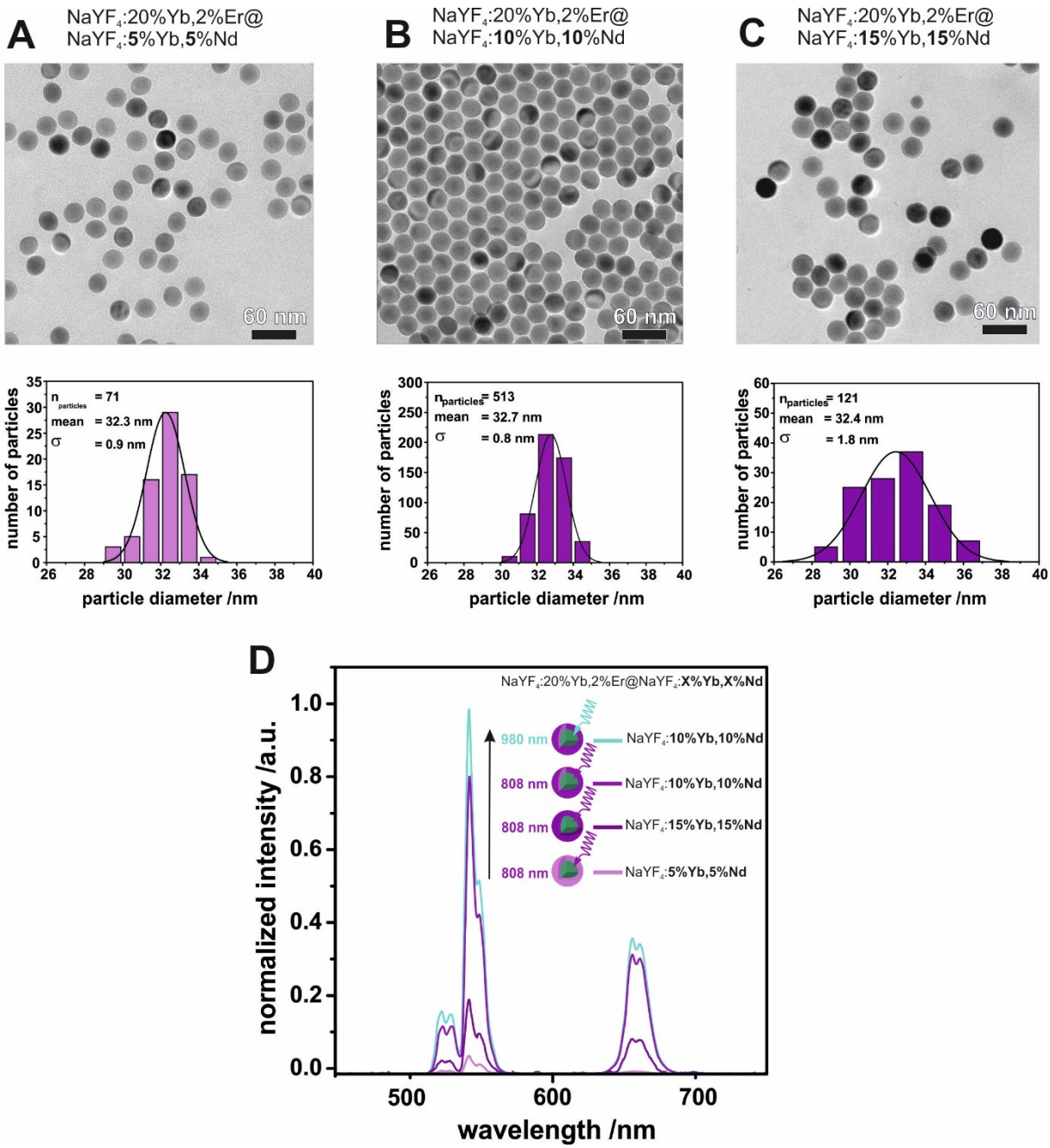

Figure S1. TEM images and size distribution of core shell particles $NaYF_4$:20%Yb,2%Er@$NaYF_4$:5%Yb,5%Nd (**A**, light purple), $NaYF_4$:20%Yb,2%Er@$NaYF_4$:10%Yb,10%Nd (**B**, purple) and $NaYF_4$:20%Yb,2%Er@$NaYF_4$:15%Yb,15%Nd (**C**, dark purple). Luminescence spectra of core-shell particles $NaYF_4$:20%Yb,2%Er@$NaYF_4$:5%Yb,5%Nd (light purple), $NaYF_4$:20%Yb,2%Er@$NaYF_4$:10%Yb,10%Nd (purple) and $NaYF_4$:20%Yb,2%Er@$NaYF_4$:15%Yb,15%Nd (dark purple) excited by 808 nm and core shell particles $NaYF_4$:20%Yb,2%Er@$NaYF_4$:10%Yb (turquoise) excited by 980 nm **(D)**. All particles are dispersed in cyclohexane. The spectra were acquired under same laser excitation power of 13 $W \cdot cm^{-2}$ and normalized to the particle concentration evaluated by ICP-MS. For the comparison the emission at 540 nm of the $NaYF_4$:20%Yb,2%Er@$NaYF_4$:10%Yb,10%Nd (turquoise) excited at 980 nm was set to one, and the spectra recorded at 808 nm excitation were corrected by the same factor.

4. Surface Modification of Upconversion Nanoparticles

The ligand exchange strategy with nitrosyl tetrafluoroborate is based on a method described by Wiesholler *et al*[1]. In a two-phase system consisting of equal volumes of cyclohexane and DMF the nanoparticles were dispersed. $NOBF_4$ (1 mg per 1 mg UCNPs) was added and the dispersion was stirred at slightly elevated temperature (~40 °C) for 10 min. During this time the oleate-capped hydrophobic UCNPs were transferred from the cyclohexane phase into the DMF phase. This phase transfer can be easily monitored by control of the upconversion luminescence via excitation with a 980 nm laser module (200 mW, cw). Surface modification is complete, when only the DMF phase exhibits upconversion luminescence. The clear upper cyclohexane phase was discarded, and the particles were precipitated by excess of chloroform. The suspension is centrifuged at 1,000 g for 5 min. The jellylike precipitate is washed twice with chloroform. Finally, the BF_4^--stabilized particles are dispersed in DMF, and aggregates were removed by centrifugation at 1,000 g for 3 min. Poly(acrylic acid) (M_W ~2,100) was dissolved in water (2 mg·mL^{-1}) and added to the BF_4^--stabilized nanoparticles dispersed in DMF. The solution was stirred and kept at a moderate temperature of 40 °C for 15 min. Afterwards the dispersion was centrifuged (13,600 g for 20 min) and washed twice with water. Finally, the supernatants were collected after centrifugation at 1,000 g for 3 min.

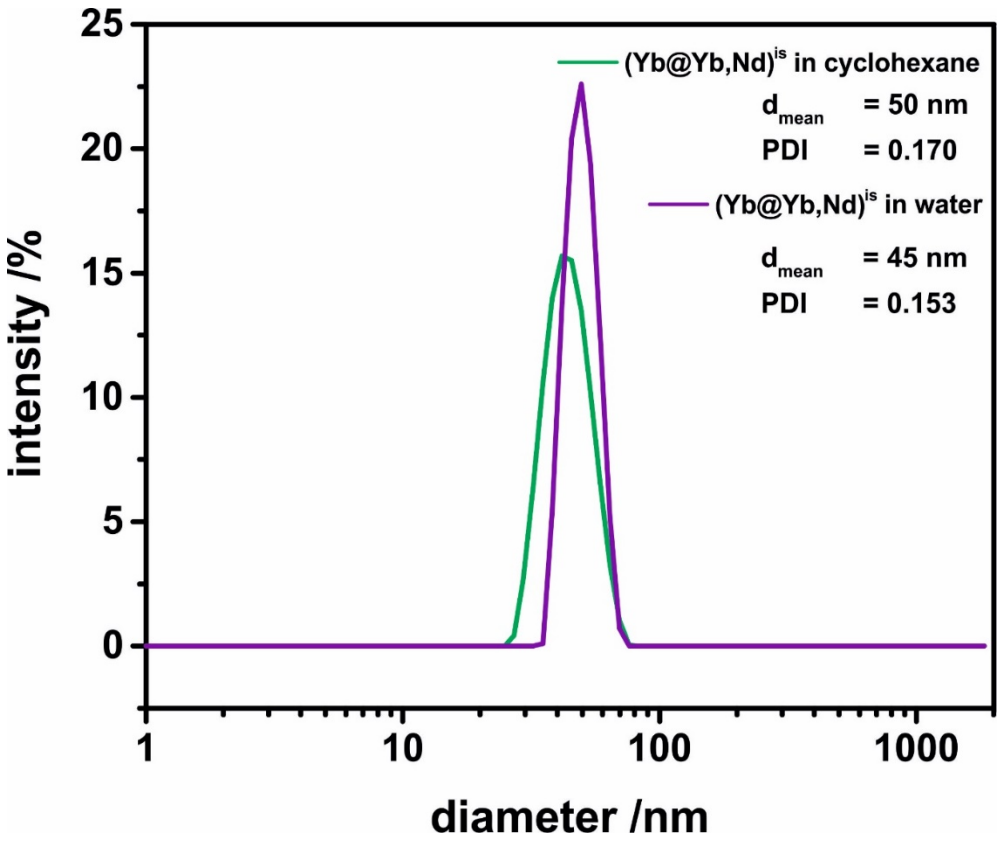

Figure S2. Colloidal stability and monodispersity of $NaYF_4$:20%Yb,2%Er@$NaYF_4$:10%Yb,10%Nd@$NaYF_4$ particles before (blue) and after surface modification with poly(acrylic acid) was confirmed by a solvodynamic diameter of 45 nm with a polydispersity index of 0.153 measured by dynamic light scattering of the particle dispersion in water (1 mg·L^{-1}). No agglomeration of the particles in dispersion over 3 months can be observed.

5. Luminescence Properties of (Yb@Yb,Nd)^{as} and (Yb@Yb,Nd)^{is} Particles Excited at 980 nm

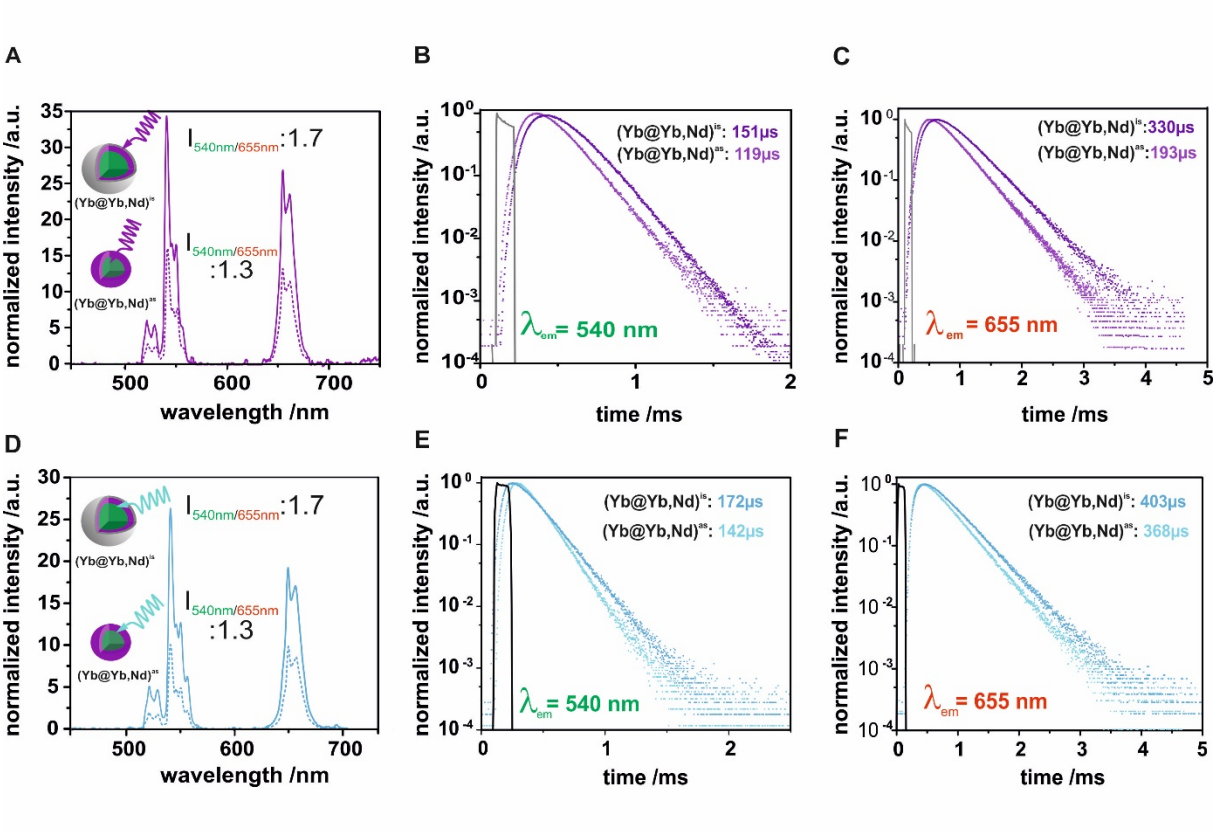

Figure S3. Luminescence spectra **(A)** and decay times for the green (540 nm) **(B)** and red (655 nm) **(C)** emission of core-shell particles $NaYF_4$:20%Yb,2%Er@$NaYF_4$:10%Yb,10%Nd (Yb@Yb,Nd)^{as} (dashed line and bright purple) and core-shell-shell particles $NaYF_4$:20%Yb,2%Er@$NaYF_4$:10%Yb,10%Nd@$NaYF_4$ (Yb@Yb,Nd)^{is} (solid line and dark purple) in aqueous solutions, excited at 808 nm (purple). The luminescence spectra **(D)** for the 980 nm (turquois) excitation and decay times for the green (540 nm) **(E)** and red (655 nm) **(F)** emission of core-shell particles $NaYF_4$:20%Yb,2%Er@$NaYF_4$:10%Yb,10%Nd (Yb@Yb,Nd) (dashed line and bright turquois) and core-shell-shell particles $NaYF_4$:20%Yb,2%Er@$NaYF_4$:10%Yb,10%Nd@$NaYF_4$ (Yb@Yb,Nd)^{is} (solid line and dark turquois) in aqueous solutions, excited at 980 nm (turquois).

6. Characterization of the Different Particle Systems used to compare 808 nm Excitation to 980 nm Excitation

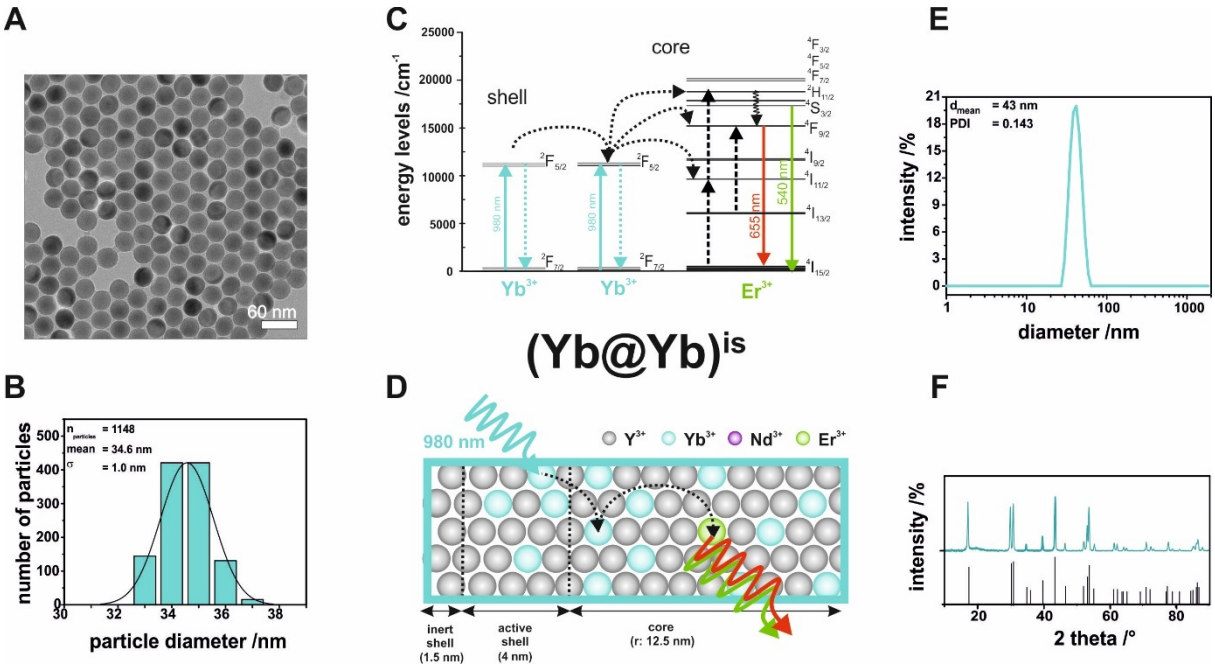

Figure S4.TEM-image **(A)** and corresponding size distribution (**B**) of $NaYF_4$:20%Yb,2%Er@$NaYF_4$:10%Yb@$NaYF_4$ particles ($(Yb@Yb)^{is}$). The diameter averaged from 1,148 particles is 34.6 ± 1.0 nm. Possible energy transfer processes **(C)** and lateral distribution of the lanthanide ions (Y^{3+}, Yb^{3+}, Nd^{3+} and Er^{3+}) in the different layers (core, active and inert shell) **(D)** are symbolized**.** The near monodispersity of the particles in aqueous solutions was confirmed by a solvodynamic diameter of 43 nm with a polydispersity index of 0.143 measured by dynamic light scattering of the particle dispersion in water (1 mg·L^{-1}). No agglomeration of the particles over 3 months in dispersion can be observed **(E).** The diffraction patterns reveal a hexagonal crystal phase as the reflexes of the nanocrystals match the standard reference pattern of β-$NaYF_4$ (ICDD PDF #16-334) (black) **(F).**

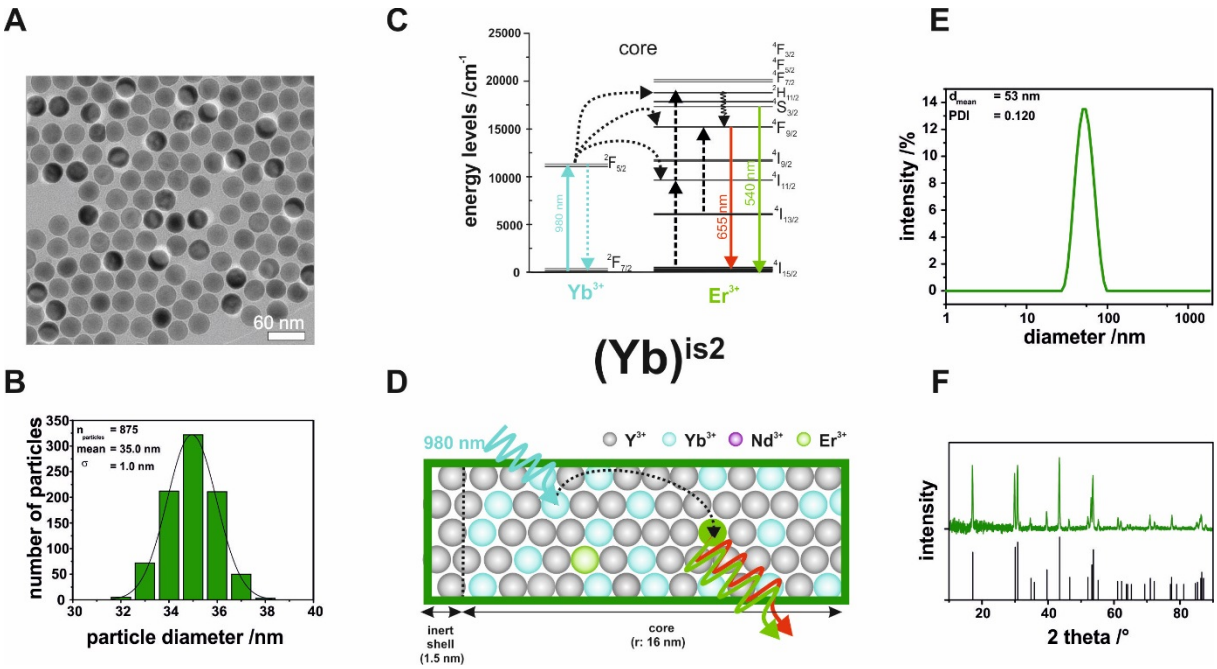

Figure S5.TEM-image **(A)** and corresponding size distribution **(B)** of $NaYF_4$(20%Yb,2%Er)@$NaYF_4$ particles ($(Yb)^{is2}$). The diameter averaged from 875 particles is 35.0 ± 1.0 nm. Possible energy transfer processes **(C)** and lateral distribution of the lanthanide ions (Y^{3+}, Yb^{3+}, Nd^{3+} and Er^{3+}) in the different layers (core, active and inert shell) **(D)** are symbolized**.** The near monodispersity of the particles in aqueous solutions was confirmed by a solvodynamic diameter of 53 nm with a polydispersity index of 0.120 measured by dynamic light scattering of the particle dispersion in water (1 mg·L^{-1}). No agglomeration of the particles in dispersion over 3 months can be observed **(E)**. The diffraction patterns reveal a hexagonal crystal phase as the reflexes of the nanocrystals match the standard reference pattern of β-$NaYF_4$ (ICDD PDF #16-334) (black) **(F).**

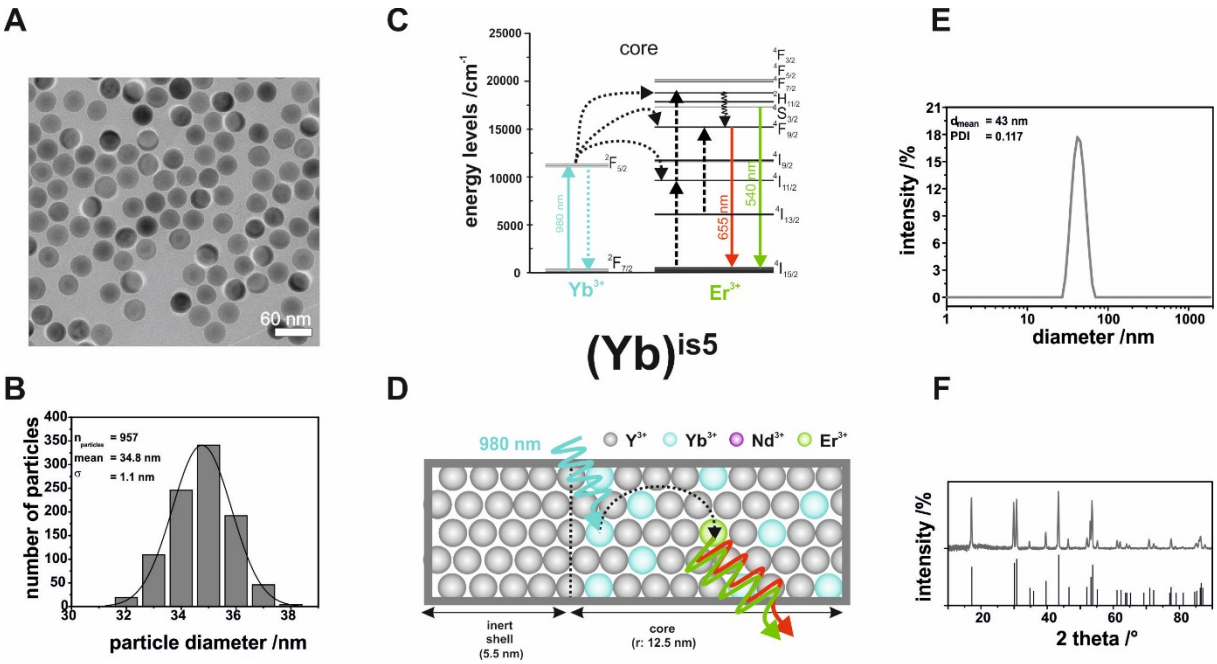

Figure S6.TEM-image **(A)** and corresponding size distribution **(B)** of $NaYF_4$(20%Yb,2%Er)@$NaYF_4$ particles ($(Yb)^{is5}$). The diameter averaged from 957 particles is 34.8 ± 1.1 nm. Possible energy transfer processes **(C)** and lateral distribution of the lanthanide ions (Y^{3+}, Yb^{3+}, Nd^{3+} and Er^{3+}) in the different layers (core, active and inert shell) **(D)** are symbolized**.** The near monodispersity of the particles in aqueous solutions was confirmed by a solvodynamic diameter of 43 nm with a polydispersity index of 0.117 measured by dynamic light scattering of the particle dispersion in water (1 mg·L^{-1}). No agglomeration of the particles over 3 months in dispersion can be observed **(E).** The diffraction patterns reveal hexagonal crystal phases as the reflexes of the nanocrystals match the standard reference pattern of β-$NaYF_4$ (ICDD PDF #16-334) (black) **(F)**.

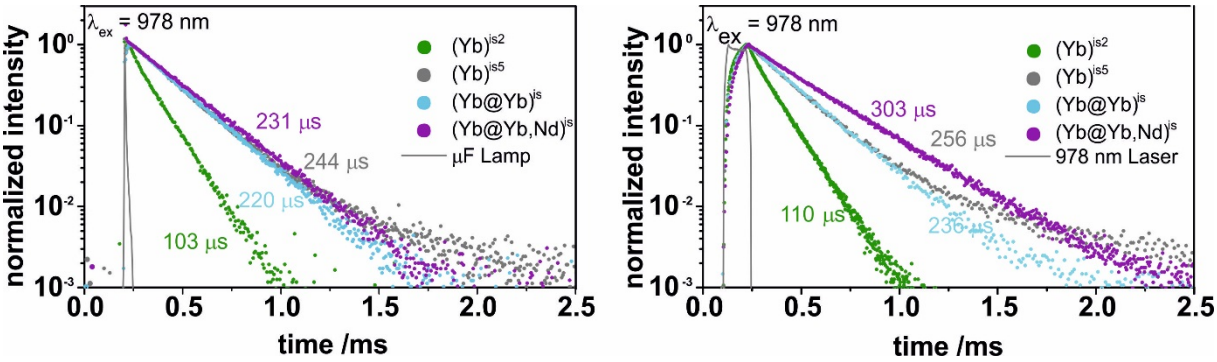

Figure S7. Decay times for the Yb emission **(A)** of particles $NaYF_4$:20%Yb,2%Er@$NaYF_4$:10%Yb,10%Nd ($(Yb@Yb,Nd)^{is}$, green), $NaYF_4$:20%Yb,2%Er@$NaYF_4$:10%Yb@$NaYF_4$ ($(Yb@Yb)^{is}$, blue), and $NaYF_4$(20%Yb,2%Er)@$NaYF_4$ particles ($(Yb)^{is2}$, black and $(Yb)^{is5}$, red) in aqueous solution under Yb excitation (978 nm) using a μFlash lamp as low-power density excitation light source and **(B)** an 8 W laser diode as high-power density light source. The intensity-weighted mean lifetimes are indicated in the graphs in the respective colors.

7. Absorption Cross-Sections Values for Nd^{3+}- and Yb^{3+}-ions

Table S2. Composition of absorption cross section values for Nd^{3+} and Yb^{3+} ions found in the literature for different host materials and excitations wavelengths.

Ln^{3+}	host material	λ_{exc} /nm	absorption cross-section / cm^2	Ref.
Nd^{3+}	LaF_3	790	$2.5 \cdot 10^{-20}$	2
Nd^{3+}	$(Gd,Y)VO_4$	808	$2 \cdot 10^{-19}$	3
Nd^{3+}	Nd^{3+}	800	$1.2 \cdot 10^{-19}$	4
Nd^{3+}	Sc_2O_3	825	$7.2 \cdot 10^{-20}$	5
Nd^{3+}	YAG*	808	$1.2 \cdot 10^{-19}$	6
Nd^{3+}	$NaYF_4$	808	10^{-14} (calculated per NP)	7
Nd^{3+}	-	~800	$\sim 10^{-19}$	8
Nd^{3+}	$NaYF_4$	805	$4.9 \cdot 10^{-20}$	this work
Nd^{3+}	$NaYF_4$	794	$1.3 \cdot 10^{-19}$	this work
Yb^{3+}	$YAlO_3$	980	$2.1 \cdot 10^{-20}$	5
Yb^{3+}	YAG*	980	$2.5 \cdot 10^{-20}$	9
Yb^{3+}	Al_2O_3	980	$1.2 \cdot 10^{-20}$	6
Yb^{3+}	-	~980	10^{-20}	8
Yb^{3+}	$NaYF_4$	978	$1.4 \cdot 10^{-20}$	this work
		976	$1.8 \cdot 10^{-20}$	this work

*Yttrium aluminium garnet

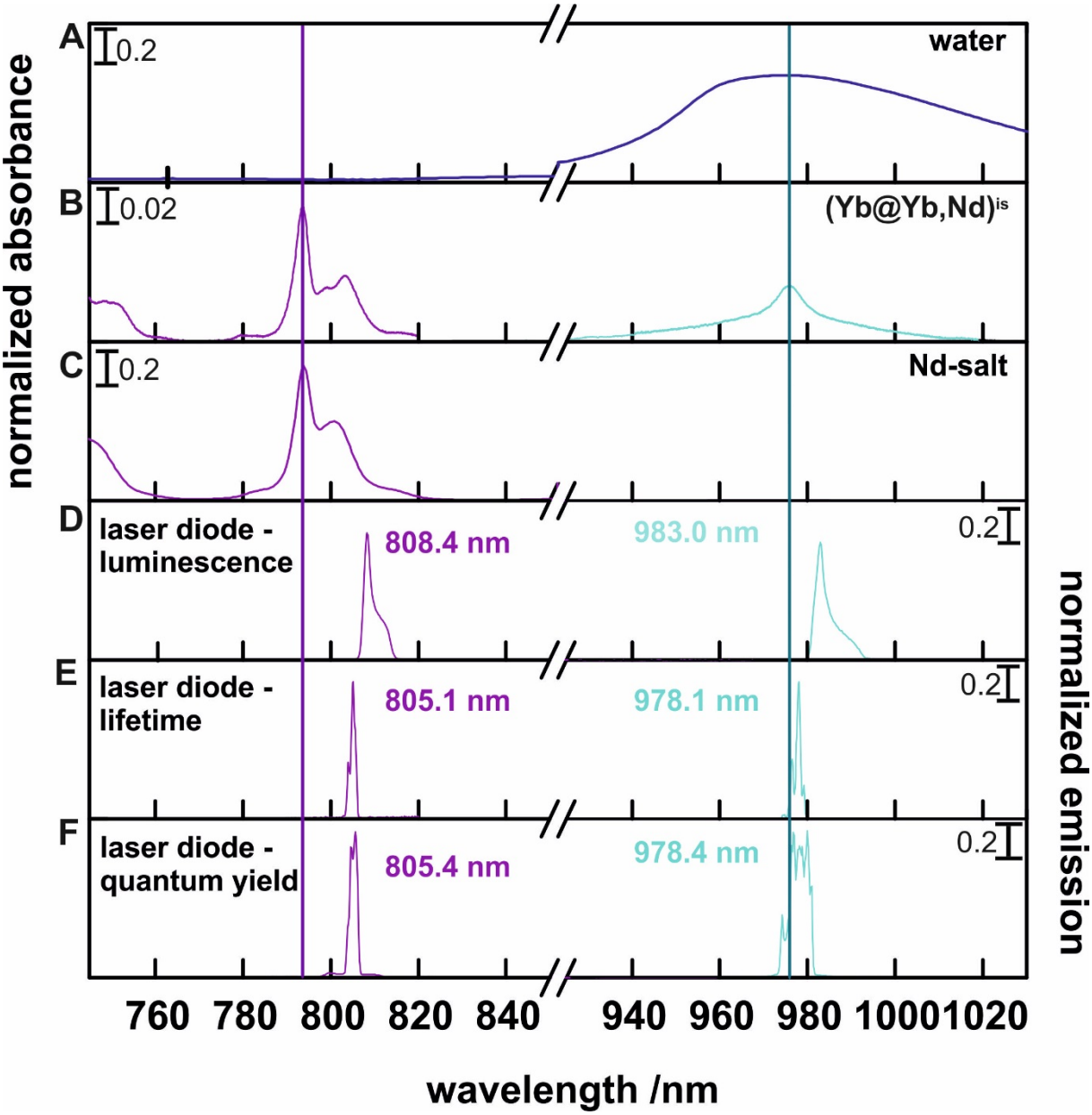

Figure S8. Absorbance spectra of water **(A)**, normalized particle cross-section of $NaYF_4$:20%Yb,2%Er@$NaYF_4$:10%Yb,10%Nd@$NaYF_4$ particles in cyclohexane **(B)** and normalized absorbance spectra of $NdCl_3$ salt (0.1 mol·L^{-1}) **(C)**. The normalized emission of the laser modules 808 nm (purple) and 980 nm (turquois) was also measured for the luminescence spectra **(D)**, lifetimes **(E)** and quantum yield measurements **(F)**. The exact values (real Nd- and Yb-excitation) for the laser excitation are listed in the Figure. The lines in purple and turquois indicate the ideal excitation wavelengths.

8. Quantum Yield Measurements

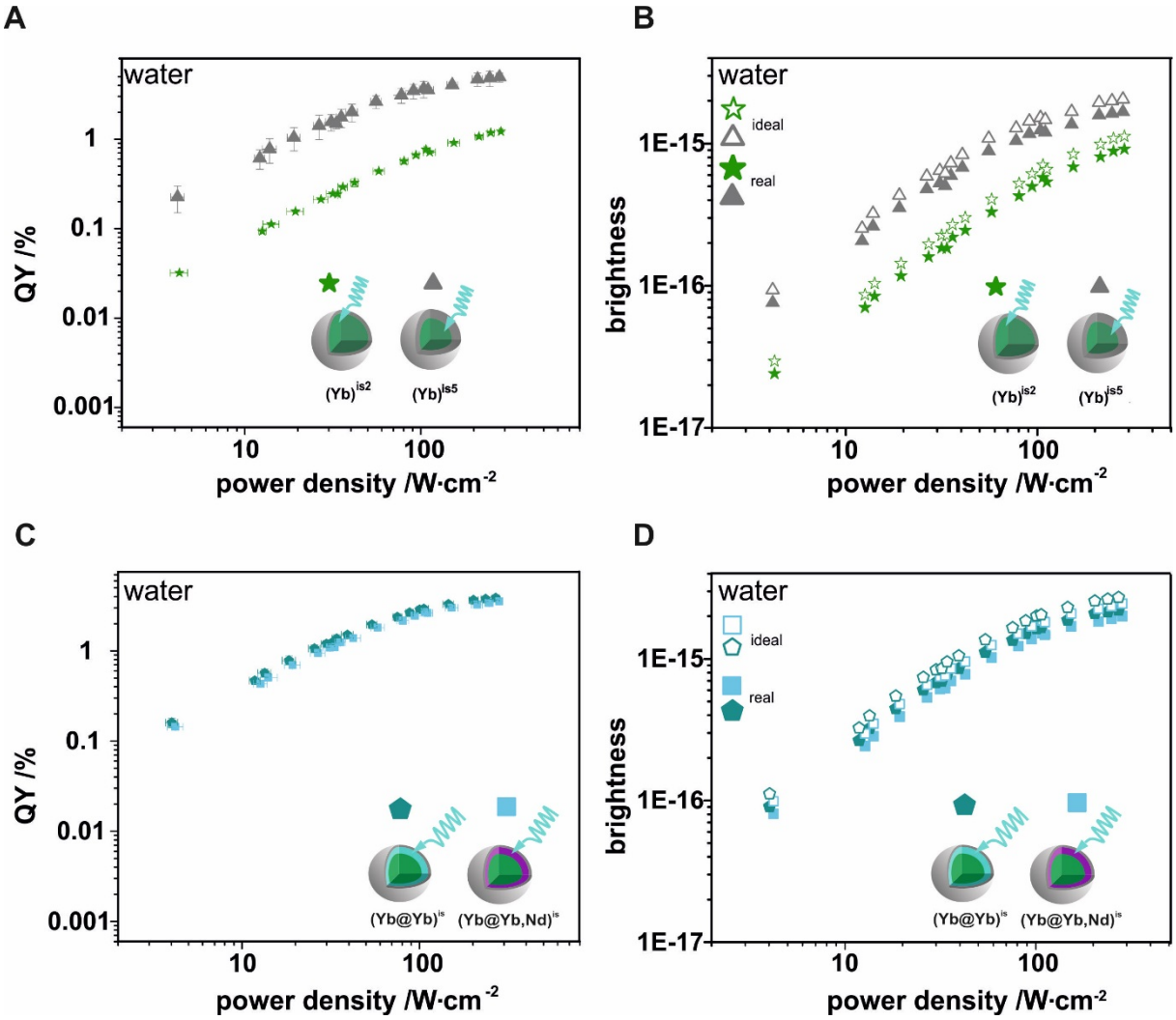

Figure S9. Power density dependent absolute quantum yields of $NaYF_4$:20%Yb,2%Er$NaYF_4$ $(Yb)^{is2}$ (green) and $(Yb)^{is5}$ (grey) particles dispersed in water at 978 nm excitation **(A).** Particle brightness in dependence of laser power of $(Yb)^{is2}$ (green) and $(Yb)^{is5}$ (grey) particles measured by excitation at 978 nm (real) in aqueous solution and calculated for an ideal excitation at 976 nm **(B).** For the particles $NaYF_4$:20%Yb,2%Er@$NaYF_4$:10%Yb@$NaYF_4$ $(Yb@Yb)^{is}$ and $NaYF_4$:20%Yb,2%Er@$NaYF_4$:10%Yb,10%Nd@$NaYF_4$ $(Yb@Nd,Yb)^{is}$ dispersed in water also power density dependent absolute quantum yield by excitation at 978 nm **(C)** and brightness caclulations **(D)** in dependence of laser power were performed. For the brightness, the ideal values for an excitation at 976 nm were also calculated. It is shown that Nd doping has no significant negative impact on Yb-excitation.

Table S3. Quantum Yield Data of the $NaYF_4$:20%Yb,2%Er@$NaYF_4$:10%Yb@$NaYF_4$ (Yb@Yb)^{is} and $NaYF_4$:20%Yb,2%Er@$NaYF_4$:10%Yb,10%Nd@$NaYF_4$ (Yb@Nd,Yb)^{is} samples in water, under 978 nm and 805 nm excitation (used in Figures 4B and 5A).

(Yb@Yb)^{is}, 978 nm		(Yb@Yb,Nd)^{is}, 978 nm		(Yb@Yb,Nd)^{is}, 805 nm	
power density /W·cm^{-2}	**quantum yield /%**	**power density /W·cm^{-2}**	**quantum yield /%**	**power density /W·cm^{-2}**	**quantum yield /%**
4.15 ± 0.36	0.225 ± 0.074	4.22 ± 0.43	0.1474 ± 0.0031	34.91 ± 0.37	0.0211 ± 0.0020
12.16 ± 0.79	0.61 ± 0.15	12.77 ± 1.14	0.444 ± 0.014	49.14 ± 0.42	0.0297 ± 0.0013
13.9 ± 1.3	0.78 ± 0.24	14.1 ± 1.8	0.520 ± 0.025	57.31 ± 0.56	0.03214 ± 0.00017
19.0 ± 1.6	1.04 ± 0.31	19.4 ± 2.0	0.71651 ± 0.00013	60.13 ± 0.76	0.03612 ± 0.00021
26.5 ± 2.0	1.42 ± 0.43	27.0 ± 2.5	0.9790 ± 0.0022	66.69 ± 0.84	0.04042 ± 0.00017
31.0 ± 2.2	1.56 ± 0.32	31.5 ± 2.8	1.12 ± 0.04	74.63 ± 0.72	0.04375 ± 0.00081
33.1 ± 1.8	1.49 ± 0.19	33.5 ± 1.4	1.137 ± 0.042	103.6 ± 1.2	0.0614 ± 0.0022
35.3 ± 2.3	1.76 ± 0.41	36.0 ± 2.4	1.2772 ± 0.0029	146.3 ± 1.5	0.0872 ± 0.0022
40.6 ± 3.1	2.01 ± 0.46	42.7 ± 4.2	1.426 ± 0.045	170.5 ± 2.6	0.1036 ± 0.0029
55.8 ± 3.9	2.63 ± 0.44	58.6 ± 5.1	1.87 ± 0.11	194.63 ± 0.61	0.12027 ± 0.00095
77.6 ± 4.4	3.10 ± 0.59	81.2 ± 6.2	2.25 ± 0.22	198.33 ± 0.21	0.1281 ± 0.0019
90.9 ± 5.1	3.47 ± 0.65	95.1 ± 4.8	2.531 ± 0.061	270.87 ± 0.25	0.17017 ± 0.00011
103.8 ± 5.5	3.68 ± 0.78	108.4 ± 2.5	2.785 ± 0.055	382.0437 ± 0.0056	0.2481 ± 0.0013
110.1 ± 8.0	3.55 ± 0.23	111.9 ± 7.5	2.71 ± 0.21	447.2 ± 1.2	0.2766 ± 0.0015
151 ± 11	4.05 ± 0.31	154 ± 13	3.11 ± 0.17	522.1 ± 1.2	0.36586 ± 0.00086
210 ± 14	4.69 ± 0.79	214 ± 16	3.368 ± 0.045		
246 ± 13	4.83 ± 0.95	249 ± 13	3.51 ± 0.10		
280 ± 13	4.95 ± 0.60	284.6 ± 4.7	3.67 ± 0.20		

Table S4. Brightness Data of the $NaYF_4$:20%Yb,2%Er@$NaYF_4$:10%Yb,10%Nd@$NaYF_4$ (Yb@Nd,Yb)[is] sample in water, under 978 nm and 805 nm excitation (real, obtained in measurement) and under 976 nm and 785 nm excitation (ideal, calculated) (used in Figure 4C).

power density /W·cm^{-2}	brightness /10^{-17} cm^2 978 nm, real	brightness /10^{-17} cm^2 976 nm, ideal	power density /W·cm^{-2}	brightness 10^{-17} cm^2 805 nm, real	brightness 10^{-17} cm^2 794 nm, ideal
4.22 ± 0.43	8.0	9.9	34.91 ± 0.37	1.46	3.71
12.8 ± 1.1	24.2	29.7	49.14 ± 0.42	2.06	5.22
14.1 ± 1.8	28.4	34.8	57.31 ± 0.56	2.23	5.66
19.4 ± 2	39.1	48.0	60.13 ± 0.76	2.51	6.36
27.0 ± 2.5	53.4	65.5	66.69 ± 0.84	2.81	7.11
31.5 ± 2.8	61.1	75	74.63 ± 0.72	3.04	7.7
33.5 ± 1.4	62.0	76	103.6 ± 1.2	4.26	10.8
36.0 ± 2.4	69.7	85	146.3 ± 1.5	6.05	15.3
42.7 ± 4.2	78	95	170.5 ± 2.6	7.2	18.2
58.6 ± 5.1	102	125	194.63 ± 0.61	8.3	21.2
81.2 ± 6.2	123	151	198.33 ± 0.21	8.9	22.5
95.1 ± 4.8	138	169	270.87 ± 0.25	11.8	30.0
108.4 ± 2.5	152	186	382.0437 ± 0.0056	17.2	43.7
111.9 ± 7.5	148	181	447.2 ± 1.2	19.2	48.7
154 ± 13	170	208	522.1 ± 1.2	25.4	64.4
214 ± 16	184	225			
249 ± 13	192	235			
284.6 ± 4.7	200	246			

Table S5. Brightness Data of the $NaYF_4$:20%Yb,2%Er@$NaYF_4$:10%Yb@$NaYF_4$ (Yb@Yb)^{is} sample in water, under 978 nm excitation (real, obtained in measurement) and under 976 nm excitation (ideal, calculated) (used in Figure 5B).

power density /W·cm^{-2}	brightness /10^{-17} cm^2 978 nm, real	brightness /10^{-17} cm^2 976 nm, ideal
4.15 ± 0.36	7.6	9.3
12.16 ± 0.79	20.7	25.4
13.9 ± 1.3	26.2	32
19.0 ± 1.6	35	43
26.5 ± 2.0	48	59
31.0 ± 2.2	53	65
33.1 ± 1.8	50	62
35.3 ± 2.3	59	73
40.6 ± 3.1	68	83
55.8 ± 3.9	89	109
77.6 ± 4.4	105	128
90.9 ± 5.1	117	144
103.8 ± 5.5	124	152
110.1 ± 8.0	120	147
151 ± 11	137	168
210 ± 14	158	194
246 ± 13	163	200
280 ± 13	167	205

9. Calculation of the $\sigma_{Ln}(\lambda_{Ex})$ and the absolute brightness

The particle brightness (B_{UC}) of an UC system is defined as the product of the total number of Ln^{3+} absorbers per nanoparticle (N_{Ln}) times the absorption cross section ($\sigma_{Ln}\ (\lambda_{Ex})\ [cm^{-2}]$) of one absorbing Ln^{3+} ion at the choosen excitation wavelength λ_{Ex} times the absolute quantum yield (Φ_{UC}).

$$B_{UC,Ln}(\lambda_{Ex}) = N_{Ln} \times \sigma_{Ln}(\lambda_{Ex}) \times \Phi_{UC}(P_{Ex}) = \sigma_{UCNP}(\lambda_{Ex}) \times \Phi_{UC}(P_{Ex}) \qquad \text{(eq. S1)}$$

The particle cross section σ_{UCNP} is controlled by the (average) particle size and (average) number of absorbing Ln^{3+} ions and their absorption cross section, which is highly sensitive to the measurement conditions and varies in literature especially for the Nd ion (Table S2). For the determination of $\sigma_{UCNP,}$ we decided to calculate the ion absorption cross section $\sigma_{Ln}(\lambda_{Ex})$ first by using a high resolution absorbance spectrum (0.2 nm spectral resolution) of the $(Yb@Yb,Nd)^{is}$ system (Figure 4A) with known NP concentration *c,* and to determine N_{Ln} subsequently.

Absorption cross section of Ln^{3+} ions $\sigma_{Ln}(\lambda_{Ex})$:

According to the Beer-Lambert law, the intensity of the incident light I_0 is reduced by passing an absorbing medium with a thickness of *d*, with cross section σ and number *n* of molecules, as follows:

$$\ln\frac{I_0}{I} = \sigma n d \qquad \text{(eq. S2a)}$$

The absorbance $A(\lambda)$ is definded by the decadic molar extincition coefficient $\varepsilon(\lambda)$, the NP concentration *c* [mol] and the sample thickness *d*,

$$A(\lambda) = \varepsilon(\lambda) c d = \log\frac{I_0}{I} \qquad \text{(eq. S2b)}$$

By combination of (eq. S2a) and (eq. S2b), we get for $\sigma_{UCNP}(\lambda_{Ex})$, with Avogadro's number N_A,

$$\sigma_{UCNP}(\lambda) = \frac{1}{\log e}\,\frac{A(\lambda)\ 10^3}{N_A\ c\ d} \qquad \text{(eq. S3)}$$

For the brightness calculation of $(Yb@Yb,Nd)^{is}$ (eq. S1) and (eq. S3) were used. Since $\sigma_{Ln}\ (\lambda_{Ex}) = \sigma_{UCNP}\ (\lambda_{Ex})/N_{Ln}$, the absorbance cross section per Ln^{3+} ion was calculated with N_{Ln} of $(Yb@Yb,Nd)^{is}$, see (Table S6B). The obtained value is listed in Table S2 and was used together with the N_{Ln} of the Nd-free systems to calculate the σ_{UCNP} and B_{UC} values of the remaining particles using (eq. 2).

Number of absorbing Ln^{3+} ions per NP:

The N_{Ln} in (eq. S1) was calculated considering the number of ions per hexagonal unit cell ($N_{unit,\ Ln}$) depending on the doping concentration (c_{Ln}) and the calculation of the number of unit cells per NP (n_{cells}) using the ratio of NP volume (V_{NP}) to unit cell volume (V_{cell}) (calculated using a method reported by Mackenzie *et al.*[10]), leading to the numbers presented in Table S6A and S6B.

Table S6. The calculated volume values of a hexagonal unit cell, of the core, the shell, and the calculated numbers of unit cells in the core, in the shell, and the number of ions per unit cell are listed for (Yb@Yb,Nd)^{is} **(A)**. The number of Yb, Er and Nd ions are given for the 4 particle systems **(B)**.

A

quantity	value
$V_{cell,\ hexagonal}$	$(1.06778 \pm 0.00471) \cdot 10^{-22}$ cm^3
$V_{NP,\ core}$	$(8.0834 \pm 0.584) \cdot 10^{-18}$ cm^3
$n_{cells,\ core}$	$(7.5703 \pm 0.5482) \cdot 10^{4}$
$V_{NP,\ shell1}$	$(1.02246 \pm 0.14653) \cdot 10^{-17}$ cm^3
$n_{cells,\ shell1}$	$(9.5755 \pm 1.3729) \cdot 10^{4}$
$V_{NP,\ shell2}$	$(4.72349 \pm 2.87756) \cdot 10^{-18}$ cm^3
$n_{cells,\ shell2}$	$(4.4236 \pm 2.6949) \cdot 10^{4}$

B

system	N_{Yb}	N_{Nd}
(Yb@Yb,Nd)^{is}	37800 ± 2700	14100 ± 2000
(Yb@Yb)^{is}	38300 ± 2800	-
(Yb)^{is2}	52100 ± 4200	-
(Yb)^{is5}	23400 ± 1700	-

10. Calculation of Intensity Change as a Function of Penetration Depth into Water

Since water shows higher absorption coefficient values (α_{H2O}) at 980 nm compared to 808 nm (Figure 4A), with deeper penetration (x) of excitation light the effective local power density (P_{Ex}) is more strongly decreased for the 980 nm excitation. With lower P_{Ex} the $\Phi_{UC}(P_{Ex})$ is also reduced, which leads to a decrease of the luminescence emission signal ($I_{UC,\,Ln}$). At a certain penetration depth (x_C) the previously stronger emission of Yb-excited UCNPs shows the same signal as the Nd-excited systems (crossing point). For $x > x_C$ the Nd-excitation will lead to a brighter emission in water than Yb-excitation (Figure 6A).

$I_{UC,\,Ln}$ depends on local P_{Ex} , the number of Ln^{3+} absorbers (N_{Ln}), the absorption cross section (σ_{Ln}) and the Φ_{UC}:

$$I_{UC,Ln}(x) \approx P_{Ex}(x) \times N_{Ln} \times \sigma_{Ln}(\lambda_{Ex}) \times \Phi_{UC}(P_{Ex}(x)) \qquad \text{(eq. S4)}$$

In an absorbing medium the passing light – here excitation light and therefore P_{Ex} - is reduced following the Beer-Lambert law:

$$P_{Ex}(x) \approx P_0 \cdot e^{-\alpha_{H2O}(\lambda_{Ex}) \cdot x} \quad , \qquad \text{(eq. S5)}$$

with $P_0 = P_{Ex}(x = 0)$. With $N_{Ln} \cdot \sigma_{Ln} \sim A_{Ln}$ it follows:

$$I_{UC,Ln}(x) \approx P_0 \cdot e^{-\alpha_{H2O}(\lambda_{Ex}) \cdot x} \times A_{Ln} \times \Phi_{UC}(P_{Ex}(x)) \qquad \text{(eq. S6)}$$

In Figure 6A the penetration depths x_C, at which the signal intensities for Yb- and Nd-excitation are equal, are determined for both real and ideal excitation at $P_0 =$ 50 W·cm^{-2}, and in Figure 6B x_C is plotted for 6 different initial power densities $P_{Ex}(x = 0) = P_0$ = 5, 50, 100, 200, 300 and 400 W·cm^{-2} for both the real and the ideal excitation. $x_C(P_0)$ is estimated from:

$$I_{UC,Yb}(x_C) = I_{UC,Nd}(x_C) \qquad \text{(eq. S7)}$$

In Figure S9 the critical penetration depth x_C varied with Nd doping concentration c_{Nd} (N_{Nd}) was calculated for ideal and real excitation at P_0 = 50 W·cm^{-2}. Since $I_{UC,\,Ln}$ scales linearly with N_{Nd} the change in c_{Nd} has a linear effect on $I_{UC,\,Nd}$. The increase in $I_{UC,\,Nd}$ with higher c_{Nd} shifts the crossing point of signal intensities for Yb- and Nd-excitation to lower depths x_C.

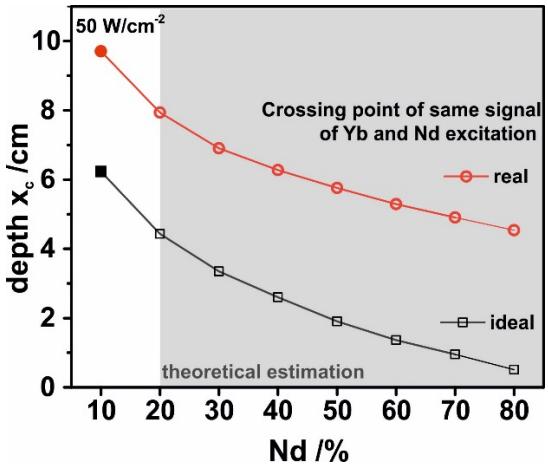

Figure S9. Calculation of the penetration depth x_C in water for a change in Nd^{3+} doping concentration of $NaYF_4$:20%Yb,2%Er@$NaYF_4$:10%Yb,10%Nd@$NaYF_4$ ((Yb@Yb,Nd)^{is}) varied from 10% up to theoretically 80% at 50 W·cm^{-2}.

For this calculation no influences by cross relaxation due to the shorter ionic distances as well as lattice strain resulting from the different ionic radii of Nd and Y, which could alter the crystal structure and result in defects at the interface, are considered.

11. Studies of the Penetration Depth in Phantom Tissue

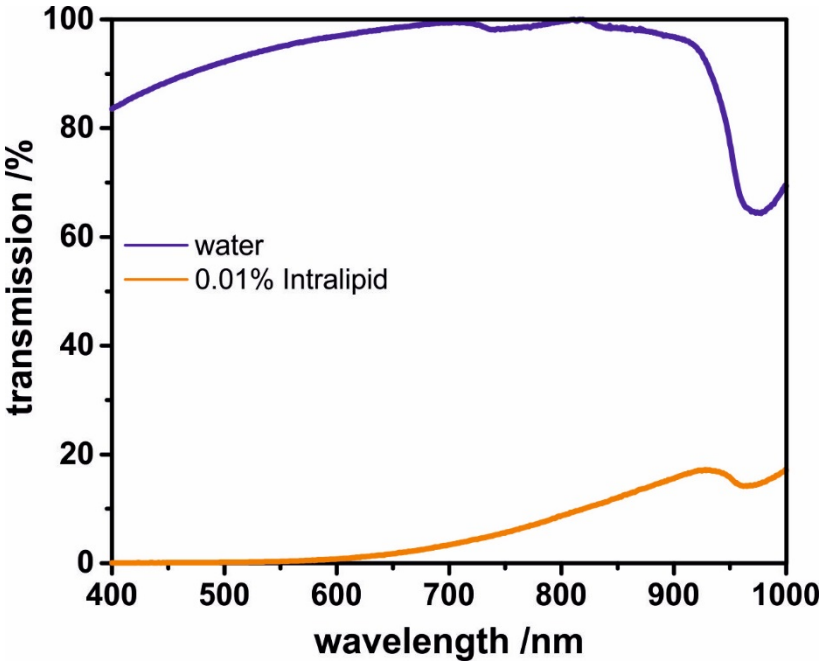

Figure S10. Transmission measurements of water and a 0.01% Intralipid emulsion. Due to large scattering of the intralipid emulsion, a 100-times dilution was used compared to the penetration depth measurements.

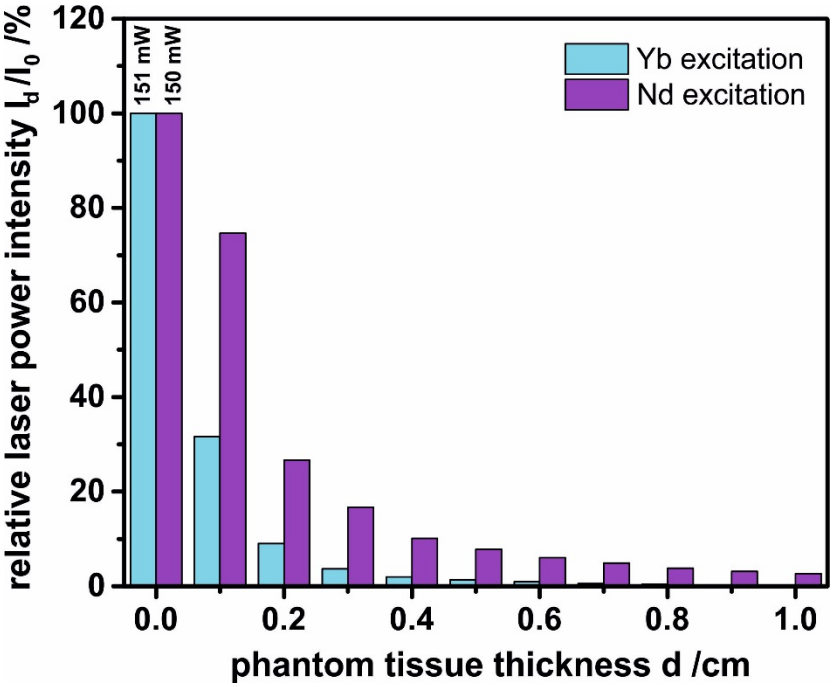

Figure S11. Decrease of the 808 nm laser power presented in purple and the 980 nm laser power presented in turquoise when propagating through an intralipid emulsion (1%) with increasing thickness from 0 - 1 cm.

12. References

[1] Wiesholler LM, Genslein C, Schroter A, Hirsch T. Plasmonic enhancement of NIR to UV upconversion by a nanoengineered interface consisting of $NaYF_4$:Yb,Tm nanoparticles and a gold nanotriangle array for optical detection of vitamin B12 in serum. Analytical Chemistry. 2018 Nov 15;90(24):14247-54.

[2] Bhutta T, Chardon AM, Shepherd DP, Daran E, Serrano C, Munoz-Yague A. Low phonon energy, Nd: LaF_3 channel waveguide lasers fabricated by molecular beam epitaxy. IEEE Journal of Quantum Electronics. 2001 Nov;37(11):1469-77.

[3] del Rosal B, Pérez-Delgado A, Carrasco E, Jovanović DJ, Dramićanin MD, Dražić G, de la Fuente ÁJ, Sanz-Rodriguez F, Jaque D. Neodymium-based stoichiometric ultrasmall nanoparticles for multifunctional deep-tissue photothermal therapy. Advanced Optical Materials. 2016 May;4(5):782-9.

[4] Estebanez N, Ferrera-González J, Francés-Soriano L, Arenal R, González-Béjar M, Pérez-Prieto J. Breaking the Nd^{3+}-sensitized upconversion nanoparticles myth about the need of onion-layered structures. Nanoscale. 2018;10(26):12297-301.

[5] Lupei V, Lupei A, Ikesue A. Transparent Nd and (Nd, Yb)-doped Sc_2O_3 ceramics as potential new laser materials. Applied Physics Letters. 2005 Mar 14;86(11):111118.

[6] Wang YF, Liu GY, Sun LD, Xiao JW, Zhou JC, Yan CH. Nd^{3+}-sensitized upconversion nanophosphors: efficient in vivo bioimaging probes with minimized heating effect. ACS Nano. 2013 Jul 23;7(8):7200-6.

[7] Jaque D, Maestro LM, Del Rosal B, Haro-Gonzalez P, Benayas A, Plaza JL, Rodriguez EM, Sole JG. Nanoparticles for photothermal therapies. Nanoscale. 2014;6(16):9494-530.

[8] del Rosal B, Rocha U, Ximendes EC, Rodríguez EM, Jaque D, Solé JG. Nd^{3+} ions in nanomedicine: Perspectives and applications. Optical Materials. 2017 Jan 1;63:185-96.

[9] Lupei V, Lupei A, Gheorghe C, Ikesue A. Sensitized Yb^{3+} emission in (Nd, Yb):$Y_3Al_5O_{12}$ transparent ceramics. Journal of Applied Physics. 2010 Dec 15;108(12):123112.

[10] Mackenzie LE, Goode JA, Vakurov A, Nampi PP, Saha S, Jose G, Millner PA. The theoretical molecular weight of $NaYF_4$: RE upconversion nanoparticles. Scientific Reports. 2018 Jan 18;8(1):1106.